ELSEVIER

Journal of Photochemistry and Photobiology A: Chemistry 101 (1996) 257–263

Journal of PHOTOCHEMISTRY AND PHOTOBIOLOGY A: CHEMISTRY

Counterion and position-dependent methylation effects on the excited states of zinc(II) complexes with 1,10-phenanthroline

Masafumi Senoue, Takashi Iwaki, Kanekazu Seki, Mikio Yagi *

Department of Physical Chemistry, Faculty of Engineering, Yokohama National University, Tokiwadai, Hodogaya-ku, Yokohama, 240, Japan

Received 4 March 1996; accepted 9 July 1996

Abstract

Time-resolved electron paramagnetic resonance and luminescence spectra have been observed for the lowest excited states of 1,10-phenanthroline (phen), 2-methyl-1,10-phenanthroline (2-Mephen), 2,9-dimethyl-1,10-phenanthroline (2,9-Me_2phen), 4,7-Me_2phen, 5,6-Me_2phen and their Zn^{2+} complexes in rigid solutions at 77 K. The sublevel preferentially populated by intersystem crossing (ISC) is the out-of-plane sublevel in Zn-2-Mephen-Cl_2 and Zn-2,9-Me_2phen-Cl_2. The observed anisotropy in the ISC of these Zn^{2+} complexes is anomalous for the ligand-localized $^3\pi\pi^*$ state. The luminescence spectra and fluorescence lifetimes indicate that the increment of the ISC rate for the out-of-plane sublevel is responsible for the anomalous anisotropy in the ISC of these Zn^{2+} complexes.

Keywords: Electron paramagnetic resonance; Emission spectrum; Fluorescence lifetime; Triplet state; Zinc(II) complex; Methyl-1,10-phenanthroline

1. Introduction

The photophysics and photochemistry of coordination compounds have been a subject of study for many years. The nature of the lowest excited triplet (T_1) states of various coordination compounds has been studied through optically detected magnetic resonance (ODMR) [1,2] and time-resolved electron paramagnetic resonance (EPR) experiments [3–5] at low temperatures. 1,10-phenanthroline (phen) is a typical bidentate chelating agent for metal ions. The T_1 state of the Zn^{2+} complex with phen is well known to possess a phen-localized $^3\pi\pi^*$ T_1 state [6,7]. Because the Zn^{2+} ion has a $3d^{10}$ closed shell configuration and has a high ionization potential of 39.7 eV, the $d\pi^*$ states are expected to be fairly high in energy. The nature of the T_1 state of the Zn^{2+} complex with phen may usually be explained by a small perturbation of phen by Zn^{2+}. The situation is the same as that observed for the Zn^{2+} complex with 2,2′-bipyridine (bpy).

However, a remarkable change in the anisotropy of the triplet sublevel populating rates has been observed for the Zn^{2+} complex with 2,9-dimethyl-1,10-phenanthroline (2,9-Me_2phen) [4]. The sublevel preferentially populated by intersystem crossing (ISC) changes from the in-plane T_y sublevel in metal-free 2,9-Me_2phen and Zn-2,9-Me_2phen-$(ClO_4)_2$ to the out-of-plane T_x sublevel in Zn-2,9-Me_2phen-Cl_2. The observed anisotropy in the ISC of Zn-2,9-Me_2phen-Cl_2 is anomalous for a 2,9-Me_2phen-localized $^3\pi\pi^*$ T_1 state. On the other hand, the effect of coordination to Zn^{2+} ions on the anisotropic ISC of phen is very small [4].

In the present work, we have observed the steady-state and time-resolved EPR spectra of the T_1 states of phen, 2-methyl-1,10-phenanthroline (2-Mephen) 4,7-Me_2phen, 5,6-Me_2phen, 2,9-Me_2phen and their complexes with Zn^{2+} in ethanol at 77 K. The counterion and position-dependent methylation effects on the anisotropic ISC of the Zn^{2+} complex with phen are discussed. The luminescence spectra and fluorescence lifetimes have also been observed to discuss the absolute values of the triplet sublevel populating rates, because the computer simulation of the time-resolved EPR spectrum only gives the relative populating rates. The preliminary results of the time-resolved EPR experiments for phen and 2,9-Me_2phen have been given in a previous paper [4].

2. Experimental details

Phen, 2,9-Me_2phen, 5,6-Me_2phen (Tokyo Kasei G.R. Grade) and 4,7-Me_2phen (Aldrich) were purified by sublimation in vacuo. 2-Mephen was prepared by the method reported in the literature [8] and was purified with a silica

---

* Corresponding author.

PII S1010-6030(96)04452-8

gel column using ethyl acetate as an eluant, followed by sublimation in vacuo. $ZnCl_2$, $Zn(ClO_4)_2 \cdot 6H_2O$ (Soekawa Chemicals), $Zn(NO_3)_2 \cdot 6H_2O$ (Koso Chemicals) and ethanol (Wako S.S. Grade) were used without further purification. The concentrations of sample solutions were 3×10^{-4} mol dm^{-3} for phen, 2-Mephen and Me_2phens. Solutions of the complexes were prepared by addition of $ZnCl_2$, $Zn(ClO_4)_2 \cdot 6H_2O$ or $Zn(NO_3)_2 \cdot 6H_2O$ (3×10^{-3} mol dm^{-3}) and phen, 2-Mephen or Me_2phen (3×10^{-4} mol dm^{-3}) to ethanol. $ZnCl_2$(2,9-Me_2phen) was obtained by dissolving stoichiometric amounts of $ZnCl_2$ and 2,9-Me_2phen (1:1) in ethanol and purified by recrystallization from nitromethane.

The apparatus for the conventional steady-state EPR measurements were described previously [9,10]. The excitations were carried out using a Canrad-Hanovia 1 kW Xe–Hg lamp through a Toshiba UV-D33S glass filter, 5 cm of distilled water and a Copal DC-494 electromechanical shutter.

The experimental setup for the time-resolved EPR measurements is the same as that reported previously [11]. A Lumonics HE-420 excimer laser (XeCl, 308 nm) was used as the exciting light pulse source with a repetition rate of 25 Hz.

For the luminescence measurements, samples were excited at 308 nm using the Lumonics HE-420 excimer laser with a repetition rate of 45 Hz. The emissions from a sample were passed through a Jobin Yvon HR-1000 monochromator and detected by a Hamamatsu Photonics R453 photomultiplier tube.

The fluorescence decay measurements were carried out with the time-correlated single-photon-counting technique. The excitations were carried out using a mode-locked Nd:YAG laser pumped, cavity-dumped dye laser (Coherent Antares 76-s, Spectra-Physics, 375, 344S, Seiko 7800 and NEC PC-9801RX) of the Instrument Center, Institute for Molecular Science, Okazaki. The typical time width of the instrumental response function was 30 ps. Samples were excited at 308 nm using the second harmonic of the synchronously pumped dye laser (Rhodamin 6G). All measurements were carried out at 77 K.

3. Results and discussion

3.1. Zero-field splittings

Assuming the isotropic g value, the spin Hamiltonian describing the T_1 states in an external magnetic field $\boldsymbol{B}$ is taken to be

$$\begin{aligned} H &= g\mu_B \boldsymbol{B}\cdot\boldsymbol{S} + \boldsymbol{S}\cdot\boldsymbol{D}\cdot\boldsymbol{S} = g\mu_B\boldsymbol{B}\cdot\boldsymbol{S} - XS_x^2 - YS_y^2 - ZS_z^2 \\ &= g\mu_B\boldsymbol{B}\cdot\boldsymbol{S} + D[S_x^2 - (1/3)S^2] + E(S_y^2 - S_z^2) \qquad (1) \end{aligned}$$

Here, $\boldsymbol{D}$ is the zero-field splitting (ZFS) tensor with principal values of $-X$, $-Y$ and $-Z$, and D and E are the ZFS parameters. The other symbols have their usual meaning. Assuming molecular planarity in the T_1 state, the principal axes (x, y, z) of the ZFS tensor were taken to be as shown in Fig. 1. The ZFS parameters D and E are defined to be $D = -3X/2$ and $E = (Z - Y)/2$.

The steady-state EPR spectra of the T_1 states of phen, 2-Mephen, 4,7-Me_2phen, 5,6-Me_2phen, 2,9-Me_2phen and their complexes with Zn^{2+} were measured in ethanol at 77 K. The results are shown in Figs. 2 and 3. The assignment of each resonance field was carried out with the aid of the stretched PVA-film method [12]. The ZFS parameters obtained from the observed resonance fields and microwave frequencies are given in Table 1. The lifetimes of the T_1 states obtained from the decay of the steady-state EPR signals are also listed in Table 1. The ZFS parameters observed in the present work for phen, 2,9-Me_2phen and Zn-phen-$(NO_3)_2$ are in good agreement with previous steady-state EPR measurements in rigid solutions at 77 K [6,13].

We can see from Table 1 that in all cases the D values obtained are ≈ 0.1 cm^{-1} and the T_1 states have lifetimes of the order of 1 s. Therefore, the T_1 states of the complexes possess $^3\pi\pi^*$ character with the dominant contribution of the local excitation in the ligand. As is well known, T_x sublevels are the lowest in energy for $^3\pi\pi^*$ states [14]. Consequently, the order of the T_1 sublevels was determined to be T_y, T_z and T_x from the top in all cases studied. As is clearly seen in Table 1, the effect of the coordination to the Zn^{2+} ion on the ZFS of phen, 4,7-Me_2phen and 5,6-Me_2phen is very small. On the other hand, the ZFS parameter D value obtained for

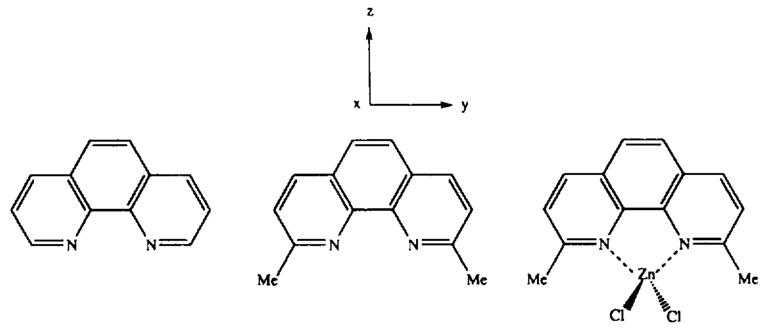

phen 2,9-Me_2phen $ZnCl_2$ (2,9-Me_2phen)

Fig. 1. Molecular structures and coordinate systems chosen for phen, 2,9-Me_2phen, and $ZnCl_2$(2,9-Me_2phen).

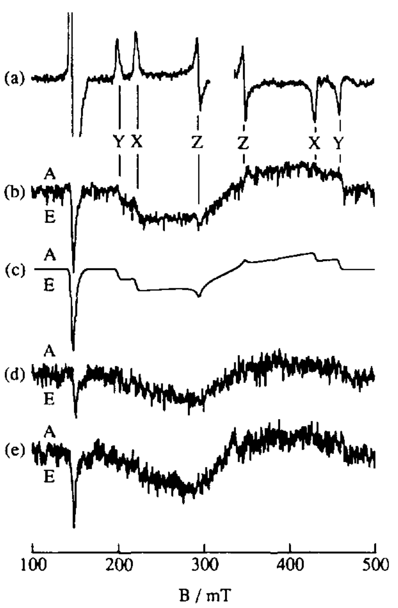

Fig. 2. (a) Steady-state and (b), (d), (e) time-resolved EPR spectra for the T_1 states of (a), (b) 5,6-Me_2phen, (d) Zn-5,6-Me_2phen-$(NO_3)_2$ and (e) Zn-5,6-Me_2phen-Cl_2 in ethanol at 77 K. The sampling times were set at 0.30–0.94 μs after the laser pulse for the time-resolved measurements. (c) Computer-simulated time-resolved EPR spectrum of 5,6-Me_2phen obtained by using $D = 0.0966$ cm^{-1}, $E = -0.0484$ cm^{-1} and P_x:P_y:P_z = 0:0.9:0.1.

Zn-2-Mephen-Cl_2 is fairly small compared with those for 2-Mephen, Zn-2-Mephen-$(NO_3)_2$ and Zn-2-Mephen-$(ClO_4)_2$. This behaviour is quite similar to that observed for the Zn^{2+} complexes with 2,9-Me_2phen. This may be due to the mixing with nearby ligand-to-ligand charge-transfer (LLCT) triplet states as suggested by Crosby and his co-workers for a series of mixed–ligand complexes with Zn^{2+} [15–17].

3.2. Relative populating rates

The time-resolved EPR spectrum of the T_1 state of 5,6-Me_2phen was measured in ethanol at 77 K, as shown in Fig. 2(b). The spectrum of the randomly oriented triplet state with spin polarization was simulated in the same manner as presented by Kottis and Lefevbre [18] with some modifications. In the present computer simulation, a Gaussian line-width of 2.5 mT was used. The polarities of the signals at the stationary fields are E,EEE/AAA from the low-field to the high-field. Here, E and A denote emission and absorption of the microwaves, respectively. The spectrum was reproduced by computer simulation resulting in the relative populating rates of P_x:P_y:P_z = 0:0.9:0.1, as shown in Fig. 2(c). The sublevel preferentially populated by ISC was found to be T_y, the top sublevel.

The time-resolved EPR spectra of the T_1 states of Zn-5,6-Me_2phen-$(NO_3)_2$ and Zn-5,6-Me_2phen-Cl_2 were measured in ethanol at 77 K, as shown in Fig. 2(d) and (e). In the same manner as for 5,6-Me_2phen, the relative populating rates were estimated to be P_x:P_y:P_z = 0:1:0 for Zn-5,6-Me_2phen-$(NO_3)_2$ and P_x:P_y:P_z = 0:0.9:0.1 for Zn-5,6-Me_2phen-Cl_2. The most notable observation is that the sublevel preferentially populated by ISC is T_y in both the metal-free ligand and the Zn^{2+} complex for 5,6-Me_2phen.

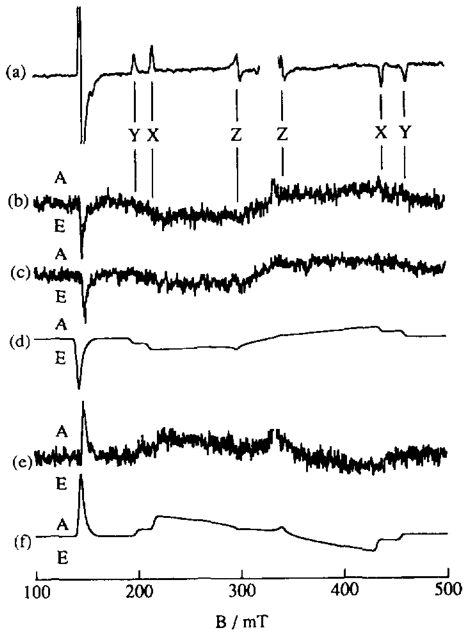

Fig. 3. (a) Steady-state and (b), (c), (e) time-resolved EPR spectra for the T_1 states of (a), (b) 2-Mephen, (c) Zn-2-Mephen-$(NO_3)_2$ and (e) Zn-2-Mephen-Cl_2 in ethanol at 77 K. The sampling times were set 0.30–0.94 μs after the laser pulse for the time-resolved measurements. (d) Computer-simulated time-resolved EPR spectrum of Zn-2-Mephen-$(NO_3)_2$ obtained by using $D = 0.1030$ cm^{-1}, $E = -0.0472$ cm^{-1} and P_x:P_y:P_z = 0:0.8:0.2 and (f) computer-simulated time-resolved EPR spectrum of Zn-2-Mephen-Cl_2 obtained by using $D = 0.1000$ cm^{-1}, $E = -0.0464$ cm^{-1} and P_x:P_y:P_z = 0.8:0.2:0.

The time-resolved EPR spectra of the T_1 states of 2-Mephen, Zn–Mephen-$(NO_3)_2$ and Zn-2-Mephen-Cl_2 were measured in ethanol at 77 K, as shown in Fig. 3(b), (c) and (e). The polarities of the signals at the stationary fields are all emissive on the low-field side and absorptive on the high-field side for 2-Mephen and Zn-2-Mephen-$(NO_3)_2$ and A,AAE/AEE for Zn-2-Mephen-Cl_2 from the low-field to the high-field. In the same manner as for 5,6-Me_2phen, the relative populating rates were estimated to be P_x:P_y:P_z = 0:0.8:0.2 for 2-Mephen and Zn-2-Mephen-$(NO_3)_2$ and P_x:P_y:P_z = 0.8:0.2:0 for Zn-2-Mephen-Cl_2, as shown in Fig. 3(d) and (f), respectively. It is interesting that the sublevel preferentially populated by ISC changes from T_y (top sublevel) in 2-Mephen and Zn-2-Mephen-$(NO_3)_2$ to T_x (bottom sublevel) in Zn-2-Mephen-Cl_2.

To examine this point more precisely, we have observed the time-resolved EPR signals of the T_1 states of the Zn^{2+} complexes with phen, 4,7-Me_2phen and 2,9-Me_2phen. The relative populating rates estimated from the computer simulations are summarized in Table 1. As is clearly seen in Table 1, the sublevel preferentially populated by ISC is T_y, the in-plane sublevel, in both the Zn^{2+} complex and the metal-free ligand for phen, 4,7-Me_2phen and 5,6-Me_2phen, as is expected for the aromatic ligand-localized $^3\pi\pi^*$ character of the Zn^{2+} complexes. On the other hand, following the coordination to Zn^{2+}, the sublevel preferentially popu-

Table 1

ZFS parameters, D and E, relative populating rates, P_i, wavenumbers of the first peak of fluorescence, ν_F, and of phosphorescence, ν_P, fluorescence lifetimes, τ_F, and phosphorescence lifetimes, τ_P, observed in ethanol at 77 K

System	D [a] (cm^{-1})	E [b] (cm^{-1})	P_x	P_y	P_z	ν_F (cm^{-1})	ν_P (cm^{-1})	τ_F (ns)	τ_P [c] (s)
phen	0.1038	−0.0491	0	0.8	0.2	29 500	22 190	2.7	1.5
Zn-phen-$(NO_3)_2$	0.1038	−0.0491	0	0.8	0.2	30 800	22 320	12.9	2.8
Zn-phen-$(ClO_4)_2$	0.1040	−0.0494	0	0.8	0.2	30 700	22 350	12.4	2.8
Zn-phen-Cl_2	0.1037	−0.0488	0	0.8	0.2	31 000	22 280	11.6	2.8
2-Mephen	0.1029	−0.0474	0	0.8	0.2	29 200	22 170	3.0	1.7
Zn-2-Mephen-$(NO_3)_2$	0.1030	−0.0472	0	0.8	0.2	28 840	22 260	13.1	3.5
Zn-2-Mephen-$(ClO_4)_2$	0.1030	−0.0473	0	0.8	0.2	28 820	22 390	13.7	3.3
Zn-2-Mephen-Cl_2	0.1000	−0.0464	0.8	0.2	0	26 900 [d]	22 100	3.3	2.5
2,9-Me_2phen	0.1026	−0.0468	0	0.7	0.3	28 900	22 170	3.0	2.2
Zn-2,9-Me_2phen-$(NO_3)_2$	0.1026	−0.0468	0	0.7	0.3	28 600	22 480	12.1	4.2
Zn-2,9-Me_2phen-$(ClO_4)_2$	0.1026	−0.0459	0	0.7	0.3	28 400	22 520	11.6	3.9
Zn-2,9-Me_2phen-Cl_2	0.1002	−0.0451	0.9	0.1	0	26 800 [d]	22 200	2.1	2.4
4,7-Me_2phen	0.0989	−0.0463	0	0.85	0.15	29 300	21 620	8.3	1.2
Zn-4,7-Me_2phen-$(NO_3)_2$	0.0998	−0.0466	0	0.7	0.3	29 500	21 800	11.3	2.6
Zn-4,7-Me_2phen-$(ClO_4)_2$	0.0997	−0.0469	0	0.7	0.3	29 900	21 820	11.4	2.7
Zn-4,7-Me_2phen-Cl_2	0.0998	−0.0468	P_y	$>P_z$	$>P_x$	30 100	21 710	12.0	2.5
5,6-Me_2phen	0.0966	−0.0484	0	0.9	0.1	27 900	21 000	6.8	1.2
Zn-5,6-Me_2phen-$(NO_3)_2$	0.0956	−0.0483	0	1.0	0	27 200	21 000 [e]	15.3	2.4
Zn-5,6-Me_2phen-$(ClO_4)_2$	0.0955	−0.0483	0	1.0	0	27 300	21 100	15.2	1.5
Zn-5,6-Me_2phen-Cl_2	0.0957	−0.0481	0	0.9	0.1	27 300	21 100 [e]	14.8	2.3

[a] $D=(-3/2)X$.

[b] $E=(Z-Y)/2$.

[c] Obtained from the decay of the steady-state EPR $\Delta M_S = \pm 1$ transition signal.

[d] Wavenumber of the first shoulder of fluorescence.

[e] Wavenumber of the first shoulder of phosphorescence.

lated changes from T_y in 2-Mephen and 2,9-Me_2phen to T_x in Zn-2-Mephen-Cl_2 and Zn-2,9-Me_2phen-Cl_2.

We should point out that the sublevel preferentially populated by ISC changes from T_y (top sublevel) in Zn-2-Mephen-$(NO_3)_2$, Zn–Mephen-$(ClO_4)_2$, Zn-2,9-Me_2phen-$(NO_3)_2$ and Zn-2,9-Me_2phen-$(ClO_4)_2$ to T_x (bottom sublevel) in Zn-2-Mephen-Cl_2 and Zn-2,9-Me_2phen-Cl_2, while it is mainly T_y in the Zn^{2+} complexes with phen, 4,7-Me_2phen and 5,6-Me_2phen studied. The replacement of the nitrate ion or the perchlorate ion by a chloride ion has a considerable influence on the anisotropy in the ISC of the Zn^{2+} complexes with 2-Mephen and 2,9-Me_2phen. As is clearly seen in Table 1, the main character of the T_1 state is the 2-Mephen-localized $^3\pi\pi^*$ in Zn-2-Mephen-$(NO_3)_2$, Zn-2-Mephen-$(ClO_4)_2$ and Zn-2-Mephen-Cl_2. The T_x sublevels are expected to be the lowest in energy and have the lowest ISC probability for $^3\pi\pi^*$ states [14,19]. However, the present time-resolved EPR study shows that the observed ISC anisotropy of Zn-2-Mephen-Cl_2 and Zn-2,9-Me_2phen-Cl_2 is anomalous for the $^3\pi\pi^*$ states of aromatic molecules.

To examine this point more precisely, we have observed the time-resolved EPR spectrum of the T_1 state of $ZnCl_2$(2,9-Me_2phen) in the crystalline state at 77 K, since the structure of Zn-2,9-Me_2phen-Cl_2 complex in solution is not known. The observed spectrum is essentially identical with that observed in ethanol at 77 K. The relative populating rates were estimated to be P_x:P_y:P_z = 0.9:0:0.1.

It should be noted that the methyl group at the phenanthroline ring position 2 plays an important role in determining the anisotropic ISC of the Zn^{2+} complex with phen. This may be related to steric hindrance between Zn^{2+} and the methyl group at the phenanthroline ring position 2. This behaviour is quite similar to that observed for the Zn^{2+} complexes with 6-methyl-2,2′-bipyridine and 6,6′-dimethyl-2,2′-bipyridine [20]. However, from the X-ray crystal analysis data, $ZnCl_2$(2,9-Me_2phen) is known to be distorted tetrahedral and 2,9-Me_2phen molecule itself is planar [21]. Assuming molecular planarity in the T_1 state, the populating rate of T_x is expected to be much smaller than those of T_y and T_z from the spin–orbit selection rule for $^3\pi\pi^*$ states [22].

In the time-resolved EPR experiments, we have no quantitative explanation for the unexpected anisotropic ISC of Zn-2-Mephen-Cl_2 and Zn-2,9-Me_2phen-Cl_2, because the computer simulation of the time-resolved EPR spectrum only gives the value of $(P_y-P_x)/(P_z-P_x)$. Further detailed investigations including the fluorescence lifetime measurements were carried out to discuss the absolute values of the triplet sublevel populating rates.

3.3. Luminescence properties

The total emission spectra of phen, 2-Mephen, 4,7-Me_2phen, 5,6-Me_2phen, 2,9-Me_2phen and their complexes with Zn^{2+} were measured in ethanol at 77 K. The results are shown in Figs. 4 and 5. The observed wavenumbers of the first peaks of fluorescence and phosphorescence are listed in Table 1. From the similarity of the fluorescence spectra between phen and phenanthrene [23], a parent hydrocarbon

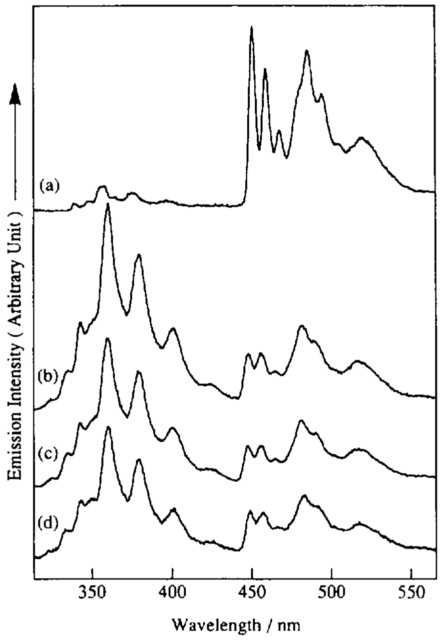

Fig. 4. (a) Emission spectra of phen, (b) Zn-phen-$(NO_3)_2$ (c) Zn-phen-$(ClO_4)_2$ and (d) Zn-phen-Cl_2 in ethanol at 77 K.

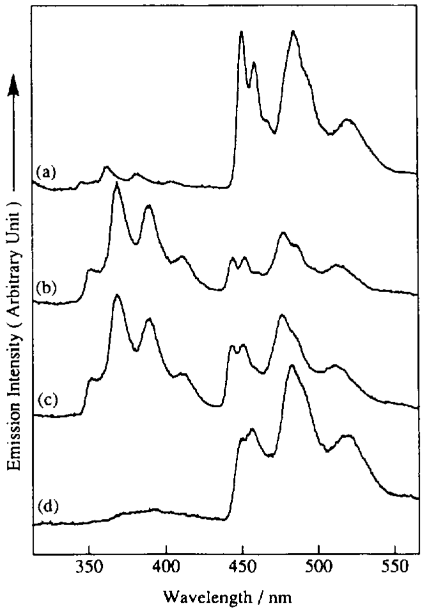

Fig. 5. (a) Emission spectra of 2,9-Me_2phen, (b) Zn-2,9-Me_2phen-$(NO_3)_2$, (c) Zn-2,9-Me_2phen-$(ClO_4)_2$ and (d) Zn-2,9-Me_2phen-Cl_2 in ethanol at 77 K.

of phen, the lowest excited singlet (S_1) state of phen is expected to possess a $^1\pi\pi^*$ character. As is seen in Table 1 and Figs. 4 and 5, the energies of the first vibronic bands and the vibrational structures of the fluorescence spectra of the Zn^{2+} complexes are similar to those of phen. Therefore, the S_1 states of the complexes possess $^1\pi\pi^*$ character with the dominant contribution of the local excitation in the ligand. However, the fluorescence spectra of Zn–Mephen-Cl_2 and Zn-2,9-Me_2phen-Cl_2 shift to lower energies than that of phen and show blurred vibrational structure.

For 2-Mephen and 2,9-Me_2phen, the intensity ratio of fluorescence to phosphorescence for the $ZnCl_2$ complex is smaller than those for the $Zn(NO_3)_2$ and $Zn(ClO_4)_2$ complexes, as shown in Fig. 5. On the other hand, the effect of counterion on the intensity ratio of fluorescence to phosphorescence is very small for the Zn^{2+} complexes with phen, 4,7-Me_2phen and 5,6-Me_2phen, as shown in Fig. 4. The observed effects of the chloride ion on the luminescence properties of the Zn^{2+} complexes with 2-Mephen and 2,9-Me_2phen may be explained by an increment of the $S_1 \rightarrow T_1$ ISC rate.

To examine this point more precisely, we have observed the fluorescence lifetimes of the Zn^{2+} complexes with various counterions in ethanol at 77 K. The results are given in Table 1. The fluorescence lifetime of phenanthrene has been reported to be 63 ns in EPA at 77 K [24]. The observed fluorescence lifetime of phen is much shorter than that of phenanthrene. Although we do not have quantitative data of the fluorescence and $S_1 \rightarrow T_1$ ISC yields, the ISC of phen is expected to be much faster than that of phenanthrene. This fast ISC is typical of *N*-heterocyclics possessing $S_1(\pi\pi^*)$ states with a close-lying $^1n\pi^*$ state [25].

For 2-Mephen and 2,9-Me_2phen, the fluorescence lifetime of the $ZnCl_2$ complex is shorter than those of the $Zn(NO_3)_2$ and $Zn(ClO_4)_2$ complexes. On the other hand, the effect of counterion on the fluorescence lifetime is very small for the Zn^{2+} complexes with phen, 4,7-Me_2phen and 5,6-Me_2phen. This means that the observed effects of the chloride ion on the fluorescence lifetimes and the above mentioned luminescence properties of the Zn^{2+} complexes with 2-Mephen and 2,9-Me_2phen can be explained by an increment of the $S_1 \rightarrow T_1$ ISC rate. Therefore the observed anomalous anisotropy in the ISC of these Zn^{2+} complexes is expected considering the increment of the ISC rate for the out-of-plane sublevel. It should be noted that the methyl group at the phenanthroline ring position 2 plays an important role in determining not only the anisotropic ISC but also the luminescence properties of the Zn^{2+} complex with phen.

3.4. Nature of the S_1 and T_1 states of metal-free phen

The symmetry of metal-free phen is considered to belong to the C_{2v} point group [26]. The S_1 and T_1 states of phen have been assigned to $^1A_1(\pi\pi^*)$ [27] and $^3B_2(\pi\pi^*)$ [28], respectively. Two configurations are involved in the T_1 state since phen has close-lying π_{a_2} and π_{b_1}, and $\pi^*_{a_2}$ and $\pi^*_{b_1}$ orbitals [27]. The wave function for the T_1 state of phen can be expressed as follows:

$$T_1 = a(^3\pi_{b_1}\pi^*_{a_2}) + b(^3\pi_{a_2}\pi^*_{b_1}) \quad (|a| > |b|) \qquad (2)$$

T_x is predicted to be the most populated sublevel from the simple group theoretical consideration of the $S_1 \rightarrow T_1$ ISC mechanisms for the S_1, $^1A_1(\pi\pi^*)$, and T_1, $^3B_2(\pi\pi^*)$, states. However, the sublevel preferentially populated by ISC was found to be mainly T_y from the present time-resolved EPR experiment.

We tried to elucidate the observed ISC anisotropy of phen by taking the effects of the close-lying $^1n\pi^*$ state on the $S_1 \rightarrow T_1$ ISC mechanisms into consideration because the ISC between $^1n\pi^*$ and $^3\pi\pi^*$ states should be much faster than that between $^1\pi\pi^*$ and $^3\pi\pi^*$ states [19]. The symmetry of the close-lying $^1n\pi^*$ state is most probably a $^1A_2(n\pi^*)$ state or a $^1B_1(n\pi^*)$ state. The possible ISC routes are predicted as follows:

$$T_x:\quad {}^1A_2(n\pi^*) \xrightarrow{H_{vib}} {}^1A_1(\pi\pi^*) \xrightarrow{H_{so}} {}^3B_2(\pi\pi^*)$$

$$\quad {}^1A_2(n\pi^*) \xrightarrow{H_{so}} {}^3B_1(n\pi^*) \xrightarrow{H_{vib}} {}^3B_2(\pi\pi^*)$$

$$T_y: {}^1A_2(n\pi^*) \xrightarrow{H_{so}} {}^3B_2(\pi\pi^*)$$

$$T_z:\quad {}^1A_2(n\pi^*) \xrightarrow{H_{vib}} {}^1B_1(n\pi^*) \xrightarrow{H_{so}} {}^3B_2(\pi\pi^*)$$

$$\quad {}^1A_2(n\pi^*) \xrightarrow{H_{so}} {}^3A_1(\pi\pi^*) \xrightarrow{H_{vib}} {}^3B_2(\pi\pi^*)$$

$$T_x:\quad {}^1B_1(n\pi^*) \xrightarrow{H_{vib}} {}^1A_1(\pi\pi^*) \xrightarrow{H_{so}} {}^3B_2(\pi\pi^*)$$

$$\quad {}^1B_1(n\pi^*) \xrightarrow{H_{so}} {}^3A_2(n\pi^*) \xrightarrow{H_{vib}} {}^3B_2(\pi\pi^*)$$

$$T_y:\quad {}^1B_1(n\pi^*) \xrightarrow{H_{vib}} {}^1A_2(n\pi^*) \xrightarrow{H_{so}} {}^3B_2(\pi\pi^*)$$

$$\quad {}^1B_1(n\pi^*) \xrightarrow{H_{so}} {}^3A_1(\pi\pi^*) \xrightarrow{H_{vib}} {}^3B_2(\pi\pi^*)$$

$$T_z: {}^1B_1(n\pi^*) \xrightarrow{H_{so}} {}^3B_2(\pi\pi^*)$$

where H_{vib} and H_{so} denote the vibronic and spin–orbit couplings, respectively. The spin–orbit coupling between the $^1n\pi^*$ and $^3\pi\pi^*$ states are considered to be the most important one. Since both the T_y and T_z sublevels couple with $^1n\pi^*$ states with one-center spin–orbit coupling, these sublevels are predicted to be preferentially populated. The observation of $P_y > P_z > P_x$ is consistent with this picture. It should be noted that the nonradiative $T_1 \rightarrow S_0$ (ground singlet) decay rate constants of the in-plane sublevels of phen are much larger than that of the out-of-plane sublevel [28]. The contribution of the close-lying $^1n\pi^*$ states to the S_1 state is consistent with the observed luminescence property of phen descried in a previous section.

3.5. *Nature of the S_1 and T_1 states of the Zn^{2+} complexes*

From the X-ray analysis $ZnCl_2$(2,9-Me_2phen) is known to be distorted tetrahedral and 2,9-Me_2phen itself is planar [21]. The symmetry of Zn-2,9-Me_2phen-Cl_2 is considered to belong to the C_{2v} point group. Assuming molecular planarity in the S_1 and T_1 states, the populating rate of the out-of-plane sublevel is expected to be much smaller than those of the in-plane sublevels from the spin–orbit selection rule for $^3\pi\pi^*$ states [22]. We tried to discuss the unexpected counterion and position-dependent methylation effects on the excited states of Zn^{2+} complex with phen in terms of the configuration mixings between the 2,9-Me_2phen-localized $\pi\pi^*$ state and the LLCT (halogen p to 2,9-Me_2phen π^* ligand–ligand charge transfer) state as suggested by Azumi and his coworkers for the low-lying excited states of ZnX_2(phen) (X = Cl, Br, I) [28]. In this framework, the wave function for the T_1 state of Zn-2,9-Me_2phen-Cl_2 can be expressed as follows:

$$T_1 = c({}^3\pi_{b_1}\pi^*_{a_2}) + d({}^3p_{b_1}\pi^*_{a_2}) \quad (|c| > |d|) \tag{3}$$

Here, the single configuration $^3B_2(\pi_{b_1}\pi^*_{a_2})$ was assumed for the 2,9-Me_2phen-localized $^3\pi\pi^*$ configuration. The wave function for a perturbing singlet state which may couple with the T_x sublevel of the T_1 state of 2,9-Me_2phen by spin–orbit coupling is expressed as a mixture of the two configurations:

$$S_i = e({}^1\pi_{a_2}\pi^*_{a_2}) + f({}^1p_{a_2}\pi^*_{a_2}) \tag{4}$$

Considering only the one-center spin–orbit coupling integral on the chlorine atom, the matrix element related to the $S_1 \rightarrow T_1$ ISC mechanisms for the T_x sublevel can be expressed as follows:

$$\langle S_i | H_{so} | T_x \rangle \approx f^* d \langle {}^1p_{a_2}\pi^*_{a_2} | H_{so} | {}^3p_{b_1}\pi^*_{a_2} \rangle \tag{5}$$

The experimental result that the sublevel preferentially populated by ISC is T_x in Zn-2,9-Me_2phen-Cl_2 is satisfactorily interpreted by this mechanism.

The absolute value of the ZFS D parameter of a ^{3}LLCT state is expected to be much smaller than that of the 2,9-Me_2phen-localized $^3\pi\pi^*$ state because the average distance between the two unpaired electrons is large in the ^{3}LLCT state. As mentioned in the previous section, the D value of Zn-2,9-Me_2phen-Cl_2 is fairly small compared with those of 2,9-Me_2phen, Zn-2,9-Me_2phen-$(NO_3)_2$ and Zn-2,9-Me_2phen-$(ClO_4)_2$ where the sublevel preferentially populated by ISC is T_y as expected for $^3\pi\pi^*$ states. This experimental result suggests that there is a configuration mixing of the 2,9-Me_2phen-localized $^3\pi\pi^*$ state with the $^3p\pi^*$ LLCT state in the T_1 state of Zn-2,9-Me_2phen-Cl_2. This behaviour is quite similar to that observed for the Zn^{2+} complexes with 2-Mephen. The observed results that the fluorescence and phosphorescence lifetimes of Zn-2,9-Me_2phen-Cl_2 are shorter than those of Zn-2,9-Me_2phen-$(NO_3)_2$ and Zn-2,9-Me_2phen-$(ClO_4)_2$, respectively, are also expected from a consideration of the $^1p\pi^*$ and $^3p\pi^*$ states and a new direct coupling they open in spin–orbit interaction. Although the exact reason for the unexpected configuration mixing between the ligand-localized $^3\pi\pi^*$ state and the $^3p\pi^*$ LLCT state could not be found in the present work, this may be related to a decrease in the energy of the zero-order $^3p\pi^*$ LLCT state by the methylation at the phenanthroline ring position 2 that is close to the chloride ion. This is consistent with the experimental finding that the T_1 energy of the chloride complex is lower than those of the nitrate and perchlorate complexes in 2-Mephen and 2,9-Me_2phen, as shown in Table 1.

On the other hand, the configuration mixing of the ligand-localized $^3\pi\pi^*$ state with the $^3p\pi^*$ LLCT state in the T_1 state is very small for the Zn^{2+} complexes with phen, 4,7-Me_2phen and 5,6-Me_2phen, and for Zn-2-Mephen-$(NO_3)_2$, Zn-2-

Me_2phen-$(ClO_4)_2$, Zn-2,9-Me_2phen-$(NO_3)_2$ and Zn-2,9-Me_2phen-$(ClO_4)_2$. The observed result that the D values of these complexes are quite similar to those of the metal-free ligands is interpreted satisfactorily by this mechanism.

4. Conclusions

Our luminescence and time-resolved EPR experiments indicate that the S_1 and T_1 sates of the Zn^{2+} complexes with phen, 2-Mephen, 4,7-Me_2phen, 5,6-Me_2phen and 2,9-Me_2phen possess mainly the ligand-localized $\pi\pi^*$ states. The observed anomalous anisotropy in the ISC of Zn-2-Mephen-Cl_2 and Zn-2,9-Me_2phen-Cl_2 is due to the increment of the ISC rate for the out-of-plane sublevel. These results are explained in terms of the configuration mixings between the ligand-localized $\pi\pi^*$ states and the halogen p to phen π^* LLCT states in low-lying excited states.

Acknowledgements

The authors wish to thank Mr Yasuaki Deguchi and Mr Masafumi Torii of our laboratory for their help in the preliminary EPR work. They express their thanks to the Instrument Center, Institute for Molecular Science, for the use of the mode-locked Nd:YAG laser pumped, cavity-dumped dye laser. They also wish to thank Mr Kazumasa Takemura and Ms Atsuko Ikemoto of our laboratory for their help in measuring the fluorescence lifetimes. The present work was supported in part by a Grant-in-Aid for Scientific Research on Priority Area "Molecular Magnetism" (Area No.228/04242210) from the Ministry of Education, Science and Culture, Japan.

References

[1] A.L. Kamyshny, A.P. Suisalu and L.A. Aslanov, *Coord. Chem. Rev., 117* (1992) 1.

[2] S. Kimachi, S. Ikeda and T. Azumi, *J. Phys. Chem., 99* (1995) 7242.

[3] H. Levanon, *Rev. Chem. Intermed., 8* (1987) 287.

[4] M. Yagi, T. Kaneshima, M. Torii, K. Matsuo and J. Higuchi, *Chem. Phys. Lett., 197* (1992) 457.

[5] A. Regev, T. Galili, C.J. Medforth, K.M. Smith, K.M. Barkigia, J. Fajer and H. Levanon, *J. Phys. Chem., 98* (1994) 2520.

[6] G.P. Rabold and L.H. Piette, *Photochem. Photobiol., 5* (1966) 733.

[7] T. Ohno and S. Kato, *Bull. Chem. Soc. Jpn., 47* (1974) 2953.

[8] J. Pijper, H. van der Goot, H. Timmerman and W.Th. Nauta, *Eur. J. Med. Chem., 19* (1984) 399.

[9] M. Yagi, K. Makiguchi, A. Ohnuki, K. Suzuki, J. Higuchi and S. Nagase, *Bull. Chem. Soc. Jpn., 58* (1985) 252.

[10] M. Yagi, T. Kaneshima, Y. Wada, K. Tekemura and Y. Yokoyama, *J. Photochem. Photobiol. A: Chem., 84* (1994) 27.

[11] Y. Shioya, K. Mikuni, J. Higuchi and M. Yagi, *J. Phys. Chem., 98* (1994) 12 521.

[12] J. Higuchi, M. Yagi, T. Iwaki, M. Bunden, K. Tanigaki and T. Ito, *Bull. Chem. Soc. Jpn., 53* (1980) 890.

[13] J. De Jong, *J. Magn. Reson., 9* (1973) 185.

[14] M. Kinoshita, N. Iwasaki and N. Nishi, *Appl. Spectrosc. Rev., 17* (1981) 1.

[15] K.A. Truesdell and G.A. Crosby, *J. Am. Chem. Soc., 107* (1985) 1787.

[16] G.A. Crosby, R.G. Highland and K.A. Truesdell, *Coord. Chem. Rev., 64* (1985) 41.

[17] S. Ikeda, S. Yamamoto, K. Nozaki, T. Ikeyama, T. Azumi, J.A. Burt and G.A. Crosby, *J. Phys. Chem., 95* (1991) 8538.

[18] Ph. Kottis and R. Lefebvre, *J. Chem. Phys., 39* (1963) 393.

[19] M.A. El-Sayed, *Ann. Rev. Phys. Chem., 26* (1975) 235.

[20] M. Yagi, Y. Wada, K. Takemura, A. Ikemoto, T. Kaneshima and K. Seki, *Chem. Phys. Lett., 227* (1994) 261.

[21] H.S. Preston and C.H.L. Kennard, *J. Chem. Soc. A*, (1969) 1956.

[22] K. Asano, S. Aita and T. Azumi, *J. Phys. Chem., 87* (1983) 3829.

[23] G. Heinrich and H. Güsten, *Z. Phys. Chem. (NF), 118* (1979) 31.

[24] N. Kanamaru, H.R. Bhattacharjee and E.C. Lim, *Chem. Phys. Lett., 26* (1974) 174.

[25] H. Kokubun, *Bull. Chem. Soc. Jpn., 42* (1969) 919.

[26] S. Nishigaki, H. Yoshioka and K. Nakatsu, *Acta Crystallogr. B, 34* (1978) 875.

[27] T. Ito, N. Tanaka, I. Hanazaki and S. Nagakura, *Bull. Chem. Soc. Jpn., 42* (1969) 702.

[28] S. Ikeda, S. Yamamoto, T. Azumi and G.A. Crosby, *J. Phys. Chem., 96* (1992) 6593.